Gas-Phase Photodissociation of (η^5-Cyclopentadienyl)Fe(CO)$_2$R and (η^5-Indenyl)Fe(CO)$_2$R in a Molecular Beam: Competitive Loss of Alkyl Radical and Alkene Detected by Vacuum-Ultraviolet Ionization and Time-of-Flight Mass Spectrometry

Jeffrey A. Bartz,† Terence M. Barnhart, Douglas B. Galloway, L. Gregory Huey,‡ Thomas Glenewinkel-Meyer, Robert J. McMahon,* and F. Fleming Crim*

Contribution from the Department of Chemistry, University of Wisconsin-Madison, Madison, Wisconsin 53706-1396

Received March 1, 1993

Abstract: Molecular beam photofragmentation measurements on (cyclopentadienyl)(alkyl)iron compounds directly determine the relative importance of Fe–alkyl bond homolysis and β-hydride elimination. The UV photodissociation of CpFe(CO)$_2$CH$_2$CH$_3$ (**1**, Cp = η^5-cyclopentadienyl), CpFe(CO)$_2$CH$_2$CH$_2$CH$_3$ (**6**), and InFe(CO)$_2$CH$_2$CH$_2$CH$_3$ (**7**, In = η^5-indenyl) leads to extensive fragmentation under collision-free conditions, and each of the products carries away little translational energy. Fragmentation of CpFe(CO)$_2$CH$_2$CH$_3$ (**1**) produces CpFeH, CpFe, CpH, Cp, Fe, and •CH$_2$CH$_3$, as detected by vacuum-UV ionization and time-of-flight mass spectrometry. The CpFeH, CpFe, and •CH$_2$CH$_3$ fragments come from absorption of one UV photon, while CpH, Cp, and Fe come from two-photon dissociation. The presence of CpFeH suggests β-hydride elimination, but the large ionization potential of the accompanying alkene product (CH$_2$=CH$_2$) prevents its detection. Similarly, the ionization potential of CO is too large for VUV ionization in these experiments. Fragmentation of CpFe(CO)$_2$CH$_2$CH$_2$CH$_3$ (**6**) produces CpFeH, CpFe, CpH, Cp, Fe, •CH$_2$-CH$_2$CH$_3$, and the alkene product CH$_2$=CHCH$_3$, which is observable by VUV ionization. Thus, homolysis of the Fe–alkyl bond (which produces propyl radical) and β-hydride elimination (which produces propene) are competing processes in the gas phase. We estimate a ratio of propyl radical to propene of 1.5 ± 0.8. Photofragmentation of the indenyl complex (η^5-In)Fe(CO)$_2$CH$_2$CH$_2$CH$_3$ (**7**) yields a ratio of propyl radical to propene of 1.1 ± 0.6. The similarity of the ratios obtained from the η^5-cyclopentadienyl complex **6** and the η^5-indenyl complex **7** suggests that ring slippage is unimportant in the fragmentation process.

Introduction

A central goal of a study of the photodissociation of a polyatomic molecule is the identification of the primary photoproducts, since these products often reveal details of the photodissociation event and the attendant chemistry. We have implemented an approach to observing primary photodissociation products that uses vacuum-ultraviolet (VUV) photoionization along with time-of-flight mass spectrometry to identify primary photodissociation fragments.[1] We dissociate a parent molecule in a molecular beam with an ultraviolet photon and then ionize the fragments with a VUV photon. The greatest advantage to this approach is that the energy of the ionizing photon is often less than the appearance potential of fragment ions from the precursor molecules. Thus, we can observe fragments that come solely from the initial photolysis and not from subsequent dissociative ionization. Our goal is to apply this scheme to organometallic molecules in order to unravel the photodissociation processes and, perhaps, illuminate the solution-phase chemistry. Here we describe the application of molecular beam photolysis and VUV photoionization detection to a series of (cyclopentadienyl)(alkyl)iron compounds with the goal of determining the relative importance of simple bond homolysis and β-hydride elimination.

The condensed-phase photochemistry of CpFe(CO)$_2$R derivatives (Cp = η^5-cyclopentadienyl; R = alkyl, aryl) provides an array of structural transformations that occur by a variety of

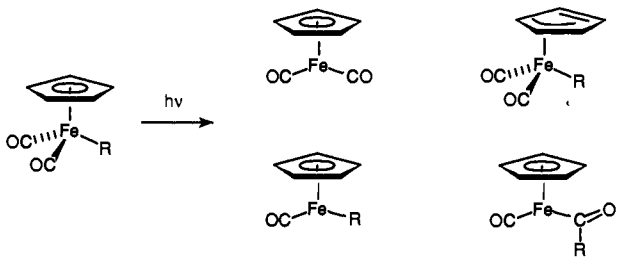

mechanisms.[2] In solution, photolysis of CpFe(CO)$_2$R in the presence of nucleophiles leads to simple substitution or rearrangement–substitution products.[2-6] In the absence of nucleophiles, photolysis produces alkanes and alkenes.[2-9] Four primary photochemical events have been invoked[2] to explain these

† Present Address: Department of Chemistry, Washington University, St. Louis, Missouri 63130-4899.

‡ Present Address: Cooperative Institute for Research in Environmental Science, University of Colorado/NOAA, Boulder, Colorado 80309-0216.

(1) Galloway, D. B.; Bartz, J. A.; Huey, L. G.; Crim, F. F. *J. Chem. Phys.* **1993**, *98*, 2107–2114.

(2) (a) Pourreau, D. B.; Geoffroy, G. L. In *Advances in Organometallic Chemistry*; Stone, F. G. A., West, R., Eds.; Academic: New York, 1985; Vol. 24, pp 249–352. (b) Gmelin, *Handbuch der Anorganischen Chemie*; Springer-Verlag: Berlin, 1984; Fe-Organische Verbindungen, Vol. B 12, pp 197–225. (c) Johnson, M. D. In *Comprehensive Organometallic Chemistry*; Wilkinson, G., Stone, F. G. A., Abel, E. W., Eds.; Pergamon: Oxford, 1982; Vol. 4, Chapter 31.2.

(3) Treichel, P. M.; Shubkin, R. L.; Barnett, K. W.; Reichard, D. *Inorg. Chem.* **1966**, *5*, 1177–1181.

(4) Su, S. R.; Wojcicki, A. *J. Organomet. Chem.* **1971**, *27*, 231–240.

(5) Alt, H. G.; Eichner, M. E.; Jansen, B. M.; Thewalt, U. *Z. Naturforsch.* **1982**, *37b*, 1109–1115.

(6) Kazlauskas, R. J.; Wrighton, M. S. *Organometallics* **1982**, *1*, 602–611.

(7) Nesmeyanov, A. V.; Chenskaya, T. B.; Babakhina, G. N.; Kritskaya, I. I. *Bull. Acad. Sci. USSR, Div. Chem. Sci. (Engl. Transl.)* **1970**, 1129–1130.

(8) Alt, H. G.; Herberhold, M.; Rausch, M. D.; Edwards, B. H. *Z. Naturforsch.* **1979**, *34b*, 1070–1077.

(9) Giese, B.; Thoma, G. *Helv. Chim. Acta* **1991**, *74*, 1143–1155.

0002-7863/93/1515-8389$04.00/0

Scheme I

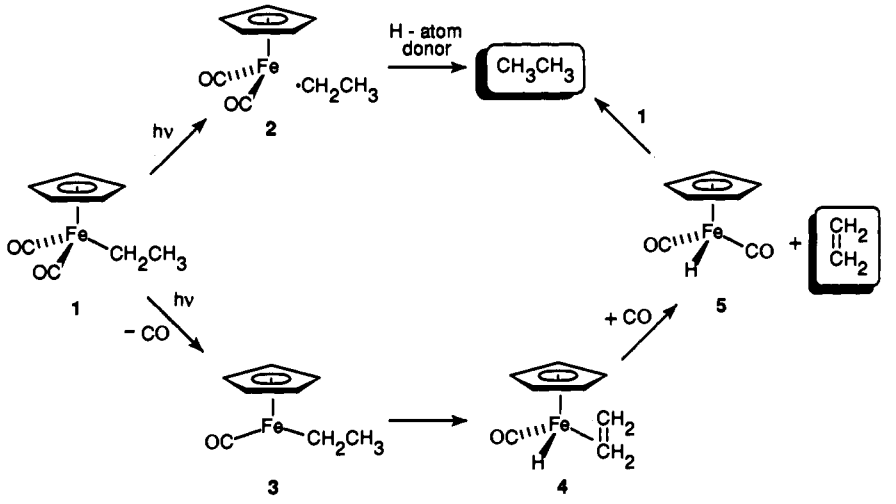

products: cleavage of the Fe–CO bond, cleavage of the Fe–R bond, migration of R from Fe to CO to form an acyl complex, Fe–(CO)R,[10] and dechelation of a portion of the η^5-Cp ring to form an η^3-Cp "ring-slipped" intermediate. Although the observed photochemistry depends on the nature of R and the experimental conditions, cleavage of the Fe–CO bond usually predominates.

When R lacks β-hydrogens (e.g., R = CH_3, CH_2Ph, Ph), a small amount of Fe–R bond homolysis apparently produces radicals that abstract hydrogen from solvent, dimerize, or add to spin traps.[7,8,11] Bond homolysis occurs more readily as radical stability increases. In the case of R = CH_2Ph, the photolysis forms $\cdot CH_2Ph$ in low quantum yield,[12] which subsequently dimerizes[12] or adds to either electron deficient alkenes[9] or spin traps.[11] The major photochemical process, however, is Fe–CO bond cleavage followed by a rapid change in hapticity from η^1-CH_2Ph to η^3-CH_2Ph.[12,13,14] When R has β-hydrogens (e.g., R = CH_2CH_3), photolysis produces both alkenes and alkanes (Scheme I). The proposed mechanism for alkene formation begins with photochemical loss of CO to produce a coordinatively unsaturated intermediate **3**.[2,6-9] Subsequent β-hydride insertion produces alkene hydride **4**. Surprisingly, neither **3** nor **4** have been detected by low-temperature matrix-isolation spectroscopy.[6,15-17] In either a solid matrix or fluid solution, the photoejected CO is believed to displace the alkene ligand of **4** to produce $CpFe(CO)_2H$ (**5**) and free alkene.[6,15,16] In solution, hydride **5** reacts with starting material **1** to produce alkane and the dimer, $[CpFe(CO)_2]_2$.[2,8] Thus, alkane formation in this system potentially occurs by at least two independent routes: cleavage of the Fe–R bond followed by hydrogen atom abstraction, and reduction of Fe–R by photogenerated Fe–H.

In this report, we describe the 280-nm photodissociation of $CpFe(CO)_2CH_2CH_3$ (**1**), $CpFe(CO)_2CH_2CH_2CH_3$ (**6**), and $InFe(CO)_2CH_2CH_2CH_3$ (**7**, In = η^5-indenyl) in a molecular beam to determine their primary photodissociation pathways. Our study demonstrates that production of both alkyl radicals and alkenes

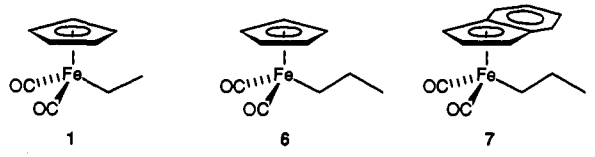

occurs in a collision-free environment by using ultraviolet (UV) photolysis, vacuum-ultraviolet (VUV) ionization, and time-of-flight mass spectrometry (TOFMS) to determine the primary photodissociation pathways. The ionization method, VUV single-photon ionization, is similar to that of other investigators,[18-21] although our method of VUV generation is different. This single-photon ionization method also differs from the detection schemes that others have used to characterize the gas-phase photochemistry of organometallic compounds, including those based on laser-induced fluorescence (LIF),[22-26] emission spectroscopy,[27-30] multiphoton ionization (MPI) mass spectrometry,[31-42] electron impact ionization mass spectrometry,[43,44] chemical trapping,[45] or transient infrared spectroscopy (TRIS).[46-51]

(10) Belt, S. T.; Ryba, D. W.; Ford, P. C. *J. Am. Chem. Soc.* **1991**, *113*, 9524–9528.
(11) Hudson, A.; Lappert, M. F.; Lednor, P. W.; MacQuitty, J. J.; Nicholson, B. D. *J. Chem. Soc., Dalton Trans.* **1981**, 2159–2162.
(12) Blaha, J. P.; Wrighton, M. S. *J. Am. Chem. Soc.* **1985**, *107*, 2694–2702.
(13) (a) Brookhart, M.; Buck, R. C. *J. Am. Chem. Soc.* **1989**, *111*, 559–567. (b) Brookhart, M.; Buck, R. C.; Danielson, E. *J. Am. Chem. Soc.* **1989**, *111*, 567–574.
(14) Herrick, R. S.; Frederick, A. B.; Duff, R. R. *Organometallics* **1989**, *8*, 1120–1121.
(15) Gerhartz, W.; Ellerhorst, G.; Dahler, P.; Eilbracht, P. *Liebigs Ann. Chem.* **1980**, 1296–1306.
(16) Mahmoud, K. A.; Rest, A. J.; Alt, H. G. *J. Chem. Soc., Dalton Trans.* **1985**, 1365.
(17) The ruthenium analog of alkene hydride **4** has been observed by matrix-isolation spectroscopy.[6,16]
(18) Feldman, D.; Laukemper, J.; Welge, K. H. *J. Chem. Phys.* **1983**, *79*, 278–282. Ruhman, S.; Haas, Y.; Laukemper, J.; Preuss, M.; Stein, H.; Feldman, D.; Welge, K. H. *J. Phys. Chem.* **1984**, *88*, 5162–5167.
(19) Schühle, U.; Pallix, J. B.; Becker, C. H. *J. Am. Chem. Soc.* **1988**, *110*, 2323–2324.
(20) Boyle, J.; Pfefferle, L. *J. Phys. Chem.* **1990**, *94*, 3336–3340.
(21) Van Bramer, S. E.; Johnston, M. V. *Anal. Chem.* **1990**, *62*, 2639–2643.
(22) $Mo(CO)_6$: Buntin, S. A.; Cavanagh, R. R.; Richter, L. J.; King, D. S. *J. Chem. Phys.* **1991**, *94*, 7937–7950.
(23) (a) $Fe(CO)_5$: Waller, I. M.; Hepburn, J. W. *J. Chem. Phys.* **1988**, *88*, 6658–6669. (b) $Ni(CO)_4$: Schlenker, F. J.; Bouchard, F.; Waller, I. M.; Hepburn, J. W. *J. Chem. Phys.* **1990**, *93*, 7110–7118.
(24) $Fe(CO)_5$: Mitchell, S. A.; Hackett, P. A. *J. Chem. Phys.* **1990**, *93*, 7813–7821.
(25) $Cu(hfac)_2$: Marinero, E. E.; Jones, C. R. *J. Chem. Phys.* **1985**, *82*, 1608–1609.
(26) $ZnMe_2$: Ishizaka, S.; Simpson, J.; Williams, J. O. *Chemtronics* **1986**, *1*, 175–177.
(27) $Mn_2(CO)_{10}$, $Mn(CO)_5Br$, $Fe(CO)_5$, (η^4-butadiene)$Fe(CO)_3$, (η^5-$C_5H_4Me)_2Fe$, $ZnMe_2$, $PbMe_4$: Karny, Z.; Naaman, R.; Zare, R. N. *Chem. Phys. Lett.* **1978**, *59*, 33–37.
(28) (a) $Cr(CO)_6$: Tyndall, G. W.; Jackson, R. L. *J. Chem. Phys.* **1988**, *89*, 1364–1377. (b) $Cr(CO)_6$, (arene)$Cr(CO)_3$, (benzene)$_2$Cr, Cp_2Cr, $Cr(hfac)_2$: Tyndall, G. W.; Larson, C. E.; Jackson, R. L. *J. Phys. Chem.* **1989**, *93*, 5508–5515. (c) Review: Jackson, R. L. *Acc. Chem. Res.* **1992**, *25*, 581–586.
(29) $Cr(CO)_6$: Cheung, N.; Yeung, E. S. *Chem. Phys. Lett.* **1992**, *189*, 164–170.
(30) $Fe(CO)_5$: Horák, D. V.; Winn, J. S. *J. Phys. Chem.* **1983**, *87*, 265–271.
(31) $Cr(CO)_6$, $Mo(CO)_6$, $Fe(CO)_5$: Duncan, M. A.; Dietz, T. G.; Smalley, R. E. *Chem. Phys.* **1979**, *44*, 415–419.
(32) Vaida, V. In *Gas Phase Inorganic Chemistry*; Russell, D. H., Ed.; Plenum: New York, 1989; pp 353–368.

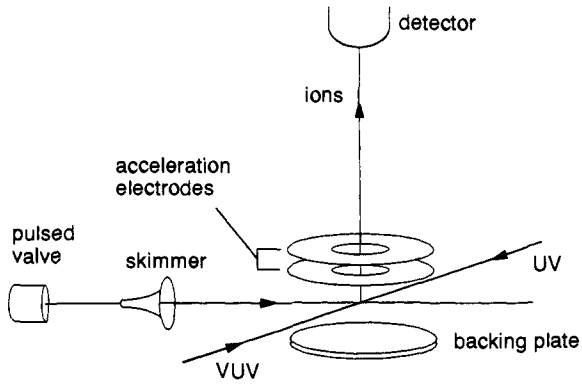

Figure 1. A portion of the experimental apparatus.

Single-photon VUV ionization using 125-nm (9.9-eV) photons is a general, energy-selective method for the ionization of primary products from photodissociation of organometallic complexes. The energy of the VUV photon limits detection to those products with ionization potentials of 9.9 eV or less. Because this energy ionizes many species near their ionization threshold, there is little excess energy for secondary dissociations. Therefore, most products detected by the mass spectrometer result from primary UV photodissociation followed by single-photon VUV ionization. Published ionization potentials[52] and other results from our laboratory[53] guide the assignment of primary photodissociation fragments.

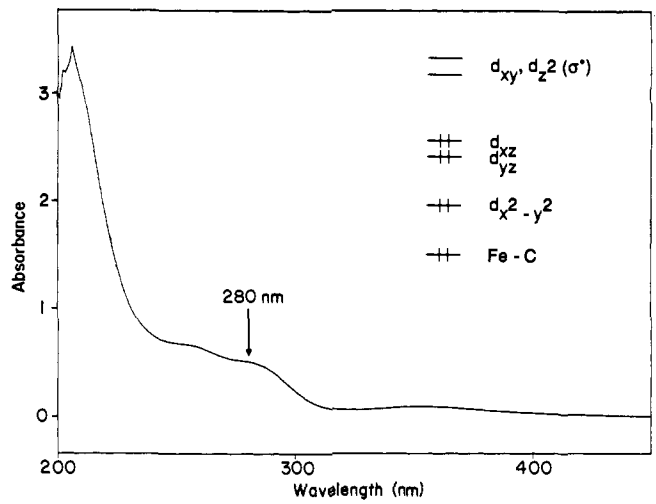

Figure 2. UV/visible absorption spectrum of CpFe(CO)$_2$CH$_2$CH$_3$ (**1**) in methylcyclohexane at 298 K. The arrow denotes the 280-nm photolysis wavelength. Inset: Frontier orbitals of **1**.

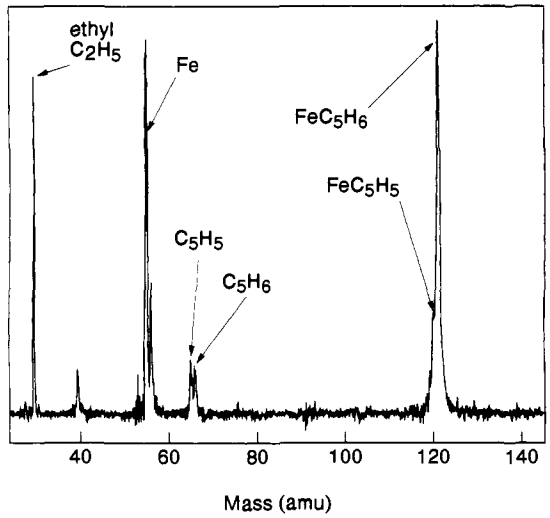

Figure 3. Mass spectrum obtained upon 280-nm photodissociation of CpFe(CO)$_2$CH$_2$CH$_3$ (**1**) followed by 125-nm ionization of the photoproducts.

Experimental Section

Synthesis of CpFe(CO)$_2$CH$_2$CH$_3$ (**1**),[54] CpFe(CO)$_2$CH$_2$CH$_2$CH$_3$ (**6**),[54] and InFe(CO)$_2$CH$_2$CH$_2$CH$_3$ (**7**)[55] followed literature procedures. Detailed information regarding the design of the molecular beam apparatus appears elsewhere.[56] Figure 1 shows a portion of the apparatus, which has two differentially pumped chambers separated by a skimmer. The organometallic compound resides in a sample reservoir, inside the molecular beam source chamber, approximately 5 cm behind the nozzle. Thermal coaxial cable heats this holder, which has an inlet for the external carrier gas, He, and an outlet that connects to the nozzle. Typically, the source chamber operates at a temperature of 80 °C and a carrier gas

(33) (a) Cr(CO)$_6$, (benzene)Cr(CO)$_3$, (benzene)$_2$Cr: Fisanick, G. J.; Gedanken, A.; Eichelberger, T. S., IV; Kuebler, N. A.; Robin, M. B. *J. Chem. Phys.* **1981**, *75*, 5215–5225. (b) HgMe$_2$: Gedanken, A.; Robin, M. B.; Kuebler, N. A. *Inorg. Chem.* **1981**, *20*, 3340–3344.

(34) (a) (arene)Cr(CO)$_3$: Hossenlopp, J. M.; Samoriski, B.; Rooney, D.; Chaiken, J. *J. Chem. Phys.* **1986**, *85*, 3331–3337. (b) Mo(CO)$_6$, (arene)Mo(CO)$_3$: Samoriski, B.; Chaiken, J. *J. Chem. Phys.* **1989**, *90*, 4079–4090. (c) (benzene)Cr(CO)$_3$: Rooney, D.; Chaiken, J. *J. Chem. Phys.* **1990**, *93*, 466–478.

(35) (a) Mo(CO)$_6$ clusters: Peifer, W. R.; Garvey, J. F. *J. Phys. Chem.* **1989**, *93*, 5906–5910; (b) Cr(CO)$_6$/MeOH heteroclusters: Peifer, W. R.; Garvey, J. F. *J. Phys. Chem.* **1991**, *95*, 1177–1183. (c) Cr(CO)$_6$: Peifer, W. R.; Garvey, J. F.; DeLeon, R. L. *J. Phys. Chem.* **1992**, *96*, 6523–6526.

(36) Fe(CO)$_5$: Nagano, Y.; Achiba, Y.; Kimura, K. *J. Chem. Phys.* **1986**, *84*, 1063–1070.

(37) Fe(CO)$_5$, (η^4-diene)Fe(CO)$_3$: (a) BelBruno, J. J.; Kobsa, P. H.; Carl, R. T.; Hughes, R. P. *J. Phys. Chem.* **1987**, *91*, 6168–6172; (b) BelBruno, J. J. *Chem. Phys. Lett.* **1989**, *160*, 267–273.

(38) Cp$_2$Fe: Liou, H. T.; Ono, Y.; Engelking, P. C.; Moseley, J. T. *J. Phys. Chem.* **1986**, *90*, 2888–2892.

(39) Cp$_2$Fe, Cp$_2$Ni: Leutwyler, S.; Even, U.; Jortner, J. *J. Phys. Chem.* **1981**, *85*, 3026–3029.

(40) (a) CpNiNO: Georgiou, S.; Wight, C. A. *J. Chem. Phys.* **1988**, *88*, 7418–7423. Co(CO)$_2$NO, Co(CO)$_2$(NO)(PR$_3$): (b) Georgiou, S.; Wight, C. A. *J. Chem. Phys.* **1989**, *90*, 1694–1700. (c) Georgiou, S.; Wight, C. A. *J. Phys. Chem.* **1990**, *94*, 4935–4940. (d) Prinslow, D. A.; Niles, S.; Wight, C. A.; Armentrout, P. B. *Chem. Phys. Lett.* **1990**, *168*, 482–488.

(41) M(β-diketonate)$_n$: Morris, J. B.; Johnston, M. V. *J. Phys. Chem.* **1985**, *89*, 5399–5401.

(42) M(acac)$_n$: Mikami, N.; Ohki, R.; Kido, H. *Chem. Phys.* **1990**, *141*, 431–440.

(43) Cr(CO)$_6$, Mo(CO)$_6$, W(CO)$_6$: Tyndall, G. W.; Jackson, R. L. *J. Chem. Phys.* **1989**, *91*, 2881–2891.

(44) (a) Fe(CO)$_5$: Ray, U.; Brandow, S. L.; Bandukwalla, G.; Venkataraman, B. K.; Zhang, Z.; Vernon, M. *J. Chem. Phys.* **1988**, *89*, 4092–4101. (b) Cp$_2$Fe: Ray, U.; Hou, H. Q.; Zhang, Z.; Schwarz, W.; Vernon, M. *J. Chem. Phys.* **1989**, *90*, 4248–4257. (c) ZnEt$_2$: Hou, H.; Zhang, Z.; Ray, U.; Vernon, M. *J. Chem. Phys.* **1990**, *92*, 1728–1746. (d) Cr(CO)$_6$, Mo(CO)$_6$, W(CO)$_6$: Venkataraman, B.; Hou, H.; Zhang, Z.; Chen, S.; Bandukwalla, G.; Vernon, M. *J. Chem. Phys.* **1990**, *92*, 5338–5362.

(45) Fe(CO)$_5$: (a) Nathanson, G.; Gitlin, B.; Rosan, A. M.; Yardley, J. T. *J. Chem. Phys.* **1981**, *74*, 361–369. (b) Yardley, J. T.; Gitlin, B.; Nathanson, G.; Rosan, A. M. *J. Chem. Phys.* **1981**, *74*, 370–378.

(46) CpRh(CO)$_2$: Wasserman, E. P.; Moore, C. B.; Bergman, R. G. *Science* **1992**, *255*, 315–318.

(47) Poliakoff, M.; Weitz, E. *Adv. Organomet. Chem.* **1986**, *25*, 277–316.

(48) Stoutland, P. O.; Dyer, R. B.; Woodruff, W. H. *Science* **1992**, *257*, 1913–1917.

(49) (a) Review: Weitz, E. *J. Phys. Chem.* **1987**, *91*, 3945–3953. (b) Ru(CO)$_5$: Bogdan, P. L.; Weitz, E. *J. Am. Chem. Soc.* **1989**, *111*, 3163–3167. (c) Os(CO)$_5$: Bogdan, P. L.; Weitz, E. *J. Am. Chem. Soc.* **1990**, *112*, 639–644.

(50) Weiller, B. H.; Grant, E. R. In *Gas Phase Inorganic Chemistry*; Russell, D. H., Ed.; Plenum: New York, 1989; pp 227–244.

(51) Cr(CO)$_6$: Fletcher, T. R.; Rosenfeld, R. N. *J. Am. Chem. Soc.* **1985**, *107*, 2203–2212.

(52) Lias, S. G.; Bartmess, J. E.; Liebman, J. F.; Holmes, J. L.; Levin, R. D.; Mallard, W. G. *Gas-Phase Ion and Neutral Thermochemistry*; American Chemical Society and American Institute of Physics: New York, 1988; Vol. 17, Suppl. 1.

(53) Huey, L. G. Ph.D. Thesis, University of Wisconsin-Madison, 1992.

(54) Davison, A.; McCleverty, J. A.; Wilkinson, G. *J. Chem. Soc.* **1963**, 1133–1138.

(55) Forschner, T. C.; Cutler, A. R. *Inorg. Chim. Acta* **1985**, *102*, 113–120.

(56) Hayden, C. C.; Penn, S. M.; Carlson-Muyskens, K. J.; Crim, F. F. *Rev. Sci. Instrum.* **1990**, *61*, 775–782.

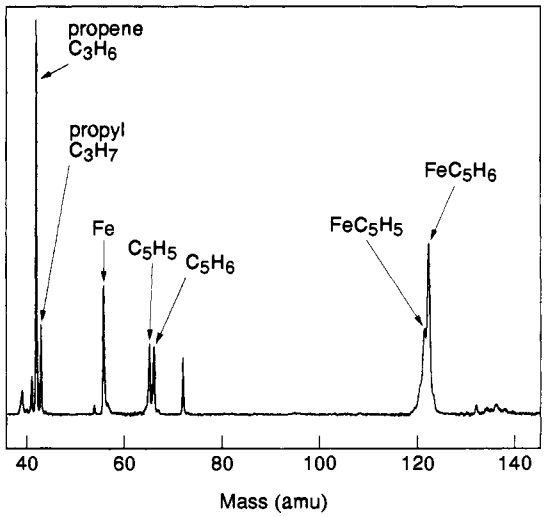

Figure 4. Mass spectrum obtained upon 280-nm photodissociation of $CpFe(CO)_2CH_2CH_2CH_3$ (**6**) followed by 125-nm ionization of the photoproducts.

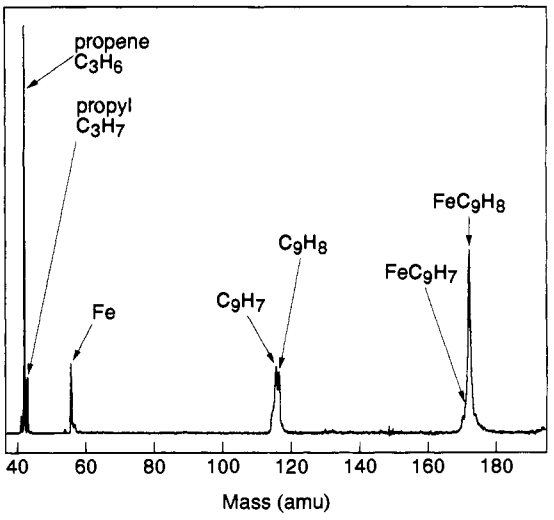

Figure 5. Mass spectrum obtained upon 280-nm photodissociation of $InFe(CO)_2CH_2CH_2CH_3$ (**7**) followed by 125-nm ionization of the photoproducts.

pressure (Matheson ultra-high purity He, 99.999%) of about 150 Torr. The nozzle pulses at 20 Hz and produces 1-μs-long bursts of gas. The valve sits in an aluminum holder, wrapped in thermal coaxial cable. Typically, the nozzle operates at 90 °C, a higher temperature than the sample reservoir, to reduce condensation or sublimation of the organometallic compound in the nozzle assembly. The seeded carrier gas travels out of the 0.5-mm nozzle and expands, producing a molecular beam that passes through a skimmer and travels into the interaction region, about 15 cm from the nozzle. In the interaction region, 280-nm UV light crosses the beam of organometallic molecules and photolyzes it. After a short time delay (0–1000 ns), 125-nm VUV light ionizes the resulting photofragments. An extraction field accelerates the ions into the field-free region of a TOFMS where they separate by mass.

The experiment uses two separate Nd:YAG-pumped dye laser systems. The first produces UV light for photolysis (280 nm) by frequency-doubling the dye laser light. The second generates VUV light by four-wave mixing in mercury. Light from the second dye laser (625 nm) passes through a KDP crystal where a portion of the beam doubles in frequency. The two wavelengths (625 nm + 312.5 nm) travel co-linearly through a lens and into a Hg heat pipe where the combination of two 312.5-nm UV photons and one 625-nm visible photon produces a single 125-nm (9.9 eV) VUV photon through resonant four-wave mixing. The details of the heat pipe design appear elsewhere.[53]

Results

A. Photodissociation. Figure 2 shows the electronic absorption spectrum of $CpFe(CO)_2CH_2CH_3$ (**1**). The literature does not contain detailed assignments for these electronic transitions, but photoelectron spectroscopy of $CpFe(CO)_2CH_3$ gives the pattern of filled orbitals shown in the figure.[2b,57] Because the lowest unoccupied orbitals are analogous to those for the isolobal systems $CpM(CO)_3$[58,59] and $M(CO)_3CH_3$,[57,60] we infer that the lowest excited state (S_1) of $CpFe(CO)_2R$ has ligand field character.[6,60,61] We do not know the nature of the excited state formed upon absorption of a 280-nm photon or whether it rapidly relaxes to either S_1 or S_0 by internal conversion prior to ligand dissociation.

The mass spectra from the 280-nm photodissociation of compounds **1**, **6**, and **7** appear in Figures 3–5, respectively. The observed fragments come from the absorption of either one or two 280-nm photons. In Figure 3, the fragments resulting from the absorption of one UV photon by $CpFe(CO)_2CH_2CH_3$ (**1**) are masses 29 (C_2H_5), 121 (FeCp), and 122 (FeCpH). The fragments appearing from the absorption of two photons include masses 56 (Fe), 65 (Cp), and 66 (CpH). In Figure 4, the one-photon fragments observed upon photolysis of $CpFe(CO)_2CH_2CH_2CH_3$ (**6**) are masses 42 (C_3H_6), 43 (C_3H_7), 121 (FeCp), and 122 (FeCpH). Two-photon fragments again include masses 56 (Fe), 65 (Cp), and 66 (CpH). Similarly, Figure 5 shows the single-photon fragments from the photolysis of $InFe(CO)_2CH_2CH_2CH_3$ (**7**): masses 42 (C_3H_6), 43 (C_3H_7), 171 (FeIn), and 172 (FeInH). The fragments arising from the absorption of two photons are masses 56 (Fe), 115 (In), and 116 (InH). We cannot observe CO, mass 28, in any of the mass spectra (Figures 3–5), since its ionization potential, 14.0 eV,[52] is greater than the energy of the VUV ionization photon (9.9 eV). Similarly, we cannot observe ethene, mass 28, in the photolysis of **1** (Figure 3) because its ionization potential, 10.5 eV,[53] is too high (Table I). In all cases, we determine the number of photons required for the production of a fragment by measuring the variation of the yield with laser pulse energy.

Table I. Heats of Reaction for Ionization and Secondary Dissociation of Relevant Compounds

reaction	$\Delta H°$, kcal mol^{-1} (eV)[a]
$CO \rightarrow CO^{\cdot+}$	323 (14.0)
$CpFe(CO)_2CH_3 \rightarrow CpFe(CO)_2CH_3^{\cdot+}$	180 (7.8)[b]
$CH_3CH_2^{\cdot} \rightarrow CH_3CH_2^{+}$	187 (8.1)
$CH_3CH_2^{\cdot} \rightarrow CH_2{=}CH_2^{\cdot+} + H^{\cdot}$	279 (12.1)[c]
$CH_2{=}CH_2 \rightarrow CH_2{=}CH_2^{\cdot+}$	242 (10.5)
$CH_3CH_2CH_2^{\cdot} \rightarrow CH_3CH_2CH_2^{+}$	187 (8.1)
$CH_3CH_2CH_2^{\cdot} \rightarrow CH_3CH{=}CH_2^{\cdot+} + H^{\cdot}$	258 (11.2)[d]
$CH_3CH{=}CH_2 \rightarrow CH_3CH{=}CH_2^{\cdot+}$	224 (9.7)

[a] All data are from ref 52, unless specified otherwise. [b] Reference 57. [c] Computed from the relationship $\Delta H° = \Delta H_f°(C_2H_4^{+}) + \Delta H_f°(H) - \Delta H_f°(C_2H_5)$ with data found in ref 52. [d] Computed from the relationship $\Delta H° = \Delta H_f°(C_3H_6^{+}) + \Delta H_f°(H) - \Delta H_f°(C_3H_7)$ with data found in ref 52.

B. Branching Ratios. Determining the relative amounts of propyl radical and propene formed in the photolysis of **6** and **7** requires that we know their detection efficiencies in our apparatus. The signal S for a particular mass is proportional to the number density of products n and their photoionization cross section σ, $S \propto n\sigma$. Although we know cross sections for neither propyl radical nor propene, we can estimate them from another measurement in our laboratory. We have detected products from

(57) (a) Lichtenberger, D. L.; Fenske, R. F. *J. Am. Chem. Soc.* **1976**, *98*, 50–63. (b) Lichtenberger, D. L.; Rai-Chaudhuri, A. *J. Am. Chem. Soc.* **1991**, *113*, 2923–2930.

(58) Hoffmann described the orbital interactions for $CpM(CO)_2 + L$.[59] In the case of $CpFe(CO)_2CH_3$, the orbital diagram is equivalent to that of $CpFe(CO)_3^{+}$ or $CpMn(CO)_3$.[57]

(59) Schilling, B. E. R.; Hoffmann, R.; Lichtenberger, D. L. *J. Am. Chem. Soc.* **1979**, *101*, 585–591.

(60) Geoffroy, G. L.; Wrighton, M. S. *Organometallic Photochemistry*; Academic: New York, 1979.

(61) (a) Alway, D. G.; Barnett, K. W. *Adv. Chem. Ser.* **1978**, *168*, 115–131. (b) Alway, D. G.; Barnett, K. W. *Inorg. Chem.* **1978**, *17*, 2826–2831.

Table II. Data Used for Branching Ratio Estimation

quantity	value
$\sigma(NO_2)^a$	$(4.1 \pm 1.2) \times 10^{-20}$ cm^2
$\sigma(C_3H_6)^b$	$(5.5 \pm 2.2) \times 10^{-18}$ cm^2
$\sigma(C_3H_7)$	$(9.4 \pm 2.8) \times 10^{-19}$ cm^2
C_3H_7/C_3H_6 signal	0.26 ± 0.03,[c] 0.19 ± 0.06[d]

[a] Reference 62. [b] Reference 53. [c] For compound **6**. [d] For compound **7**.

two distinct channels in the photolysis of 1-nitropropane:[53] one producing propyl radical and NO_2 and another producing propene. Since we know the photoionization cross section for NO_2 with 9.9-eV photons,[62] $\sigma_{NO_2} = (4.1 \pm 1.2) \times 10^{-20}$ cm^2, we can estimate the cross sections for propyl radical and propene. We expand an equal molar mixture of C_3H_6 and NO_2 and compare the corresponding signal intensities to determine the cross section for propene to be $\sigma_{C_3H_6} = (5.5 \pm 2.2) \times 10^{-18}$ cm^2. We use this value along with the propyl radical ion and propene ion signals from the photolysis of $C_3H_7NO_2$ to determine the photoionization cross

$$C_3H_7NO_2 \rightarrow C_3H_7 + NO_2$$
$$C_3H_7NO_2 \rightarrow C_3H_6 + HNO_2$$

section for C_3H_7 to be $\sigma_{C_3H_7} = (9.4 \pm 2.8) \times 10^{-19}$ cm^2. With these two cross sections, and the assumption that each ionization event produces the parent ion,[63] we determine the relative yields of propyl radical and propene to be (1.5 ± 0.8) for $CpFe(CO)_2CH_2CH_2CH_3$ (**6**) and (1.1 ± 0.6) for $InFe(CO)_2CH_2CH_2CH_3$ (**7**). Table II summarizes the data used in this calculation.

This estimate of the amount of bond homolysis, forming propyl radical, compared to β-hydride elimination, forming propene, involves several assumptions about the photoionization cross sections. First, we assume the nitropropane and iron experiments produce products with identical photoionization cross sections. The detected species in the 1-nitropropane experiment probably have more internal excitation than the identical species in the photodissociation of **6** or **7**. This difference may alter the photoionization cross sections and, thus, the detection efficiencies of propyl radical and propene in the two experiments. Second, the control experiment involving the photoionization of NO_2 and propene detects products significantly cooled in the molecular beam. These products differ from any internally excited fragments produced during the photodissociation of 1-nitropropane, **6**, or **7**. The additional differences in internal energy can also alter the photoionization cross sections and the accuracy of the branching ratio determination. Even with these limitations, the results show that the two channels are comparably important.

Discussion

The UV photolysis pulse (280 nm) leads to the important fragmentation chemistry of **1**, **6**, and **7**. In the absence of the UV photolysis pulse, VUV photoionization of **1** gives rise to some loss of CO but does not produce an ion derived from the ethyl radical ($^\bullet CH_2CH_3$, mass 29). Similarly, VUV photoionization of **6** results in partial loss of CO but does not produce ions derived from either the propyl radical ($^\bullet CH_2CH_2CH_3$, mass 43) or propene ($CH_2{=}CHCH_3$, mass 42) (Figure 6). We observe an ion corresponding to $CpFe(C_3H_5)$ (mass 162), which apparently arises as a result of loss of molecular H_2.[64] Propene formation from **6** and **7** must come from UV photolysis, because the VUV photon has insufficient energy to produce $C_3H_6^{\bullet+}$ from $^\bullet C_3H_7$ (Table I).

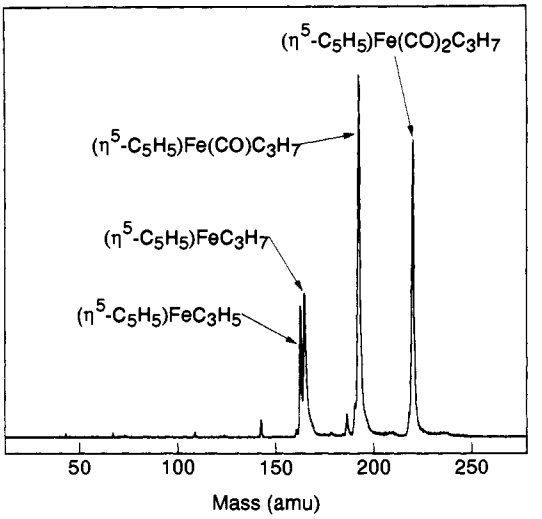

Figure 6. Mass spectrum obtained upon 125-nm ionization of $CpFe(CO)_2CH_2CH_2CH_3$ (**6**) in the absence of the 280-nm photodissociation pulse.

Table III. Approximate Bond Dissociation Energies (D) for Relevant Model Compounds

bond	D, kcal mol^{-1}	ref
Fe–CO	40	*a, b*
Fe–alkyl	30	*b, c*
$(CH_3)_2CH$–H	95	*d, e*
Fe–H	50	*b, e, f*
C=C π-bond	60	*e, g*
Fe–(η^2-$CH_2{=}CH_2$)	30	*b, h, i*

[a] Sunderlin, L. S.; Wang, D.; Squires, R. R. *J. Am. Chem. Soc.* **1992**, *114*, 2788–2796. [b] Collman, J. P.; Hegedus, L. S.; Norton, J. R.; Finke, R. G. *Principles and Applications of Organotransition Metal Chemistry*; University Science Books: Mill Valley, CA, 1987. [c] Halpern, J. *Inorg. Chim. Acta* **1985**, *100*, 41–48. [d] McMillen, D. F.; Golden, D. M. *Annu. Rev. Phys. Chem.* **1982**, *33*, 493–532. [e] Egger, K. W.; Cocks, A. T. *Helv. Chim. Acta* **1973**, *56*, 1516–1536. [f] Tilset, M.; Parker, V. D. *J. Am. Chem. Soc.* **1989**, *111*, 6711–6717. [g] Miller, S. I. *J. Chem. Educ.* **1978**, *55*, 778–780. [h] Klassen, J. K.; Selke, M.; Sorenson, A. A.; Yang, G. K. *J. Am. Chem. Soc.* **1990**, *112*, 1267–1268. [i] Buchanan, J. M.; Stryker, J. M.; Bergman, R. G. *J. Am. Chem. Soc.* **1986**, *108*, 1537–1550.

The absence of metal–carbonyl-containing species in any of our mass spectra (Figures 3, 4, and 5) shows that the combination of 280-nm photolysis and VUV photoionization ejects all CO ligands from the complex. We know that partial CO loss occurs upon VUV photoionization (Figure 6), but this pathway cannot account for the complete absence of CO ligands in the other experiments. We thus conclude that complexes **1**, **6**, and **7** must lose CO ligands following UV (280 nm) photolysis and also may lose CO ligands following VUV (125 nm) photoionization. This creates an ambiguity about the timing of CO loss, and consequently, each of the intermediates in the mechanisms described below may actually contain fewer carbonyl groups than shown in Schemes II–IV.

UV photolysis extensively fragments metal carbonyl complexes in the gas phase because there are no collisions to remove excess internal energy from the excited photofragments. Gas-phase photodissociation studies of $Fe(CO)_5$[23,45,65–67] demonstrate that absorption of a *single* UV photon produces $Fe(CO)_x$ (x = 2–4) by the loss of one or more CO ligands. Similary, single-photon photodissociation of monomeric diethylzinc ($ZnEt_2$) in the gas phase leads to loss of both alkyl substituents.[44] In our experiments, photolysis of **1**, **6**, or **7** at 280 nm provides 102 kcal/mol of excitation energy. This energy substantially exceeds the amount

(62) Nakayama, T.; Kitamura, M. Y.; Watanabe, K. *J. Chem. Phys.* **1959**, *30*, 1180–1186.
(63) The calculation actually requires only that the yield of the parent ion be the same for the two compounds.
(64) Electron impact ionization (70 eV) of $CpFe(CO)_2R$ complexes also yields H_2 elimination products: Stone, J. A.; Laycock, D. E.; Lin, M.; Baird, M. C. *J. Chem. Soc., Dalton Trans.* **1980**, 2488–2492.
(65) Whetten, R. L.; Fu, K.; Grant, E. R. *J. Chem. Phys.* **1983**, *79*, 4899–4911.
(66) Ouderkirk, A. J.; Weitz, E. *J. Chem. Phys.* **1983**, *79*, 1089–1091.
(67) Engelking, P. C. *Chem. Phys. Lett.* **1980**, *74*, 207–210.

Scheme II

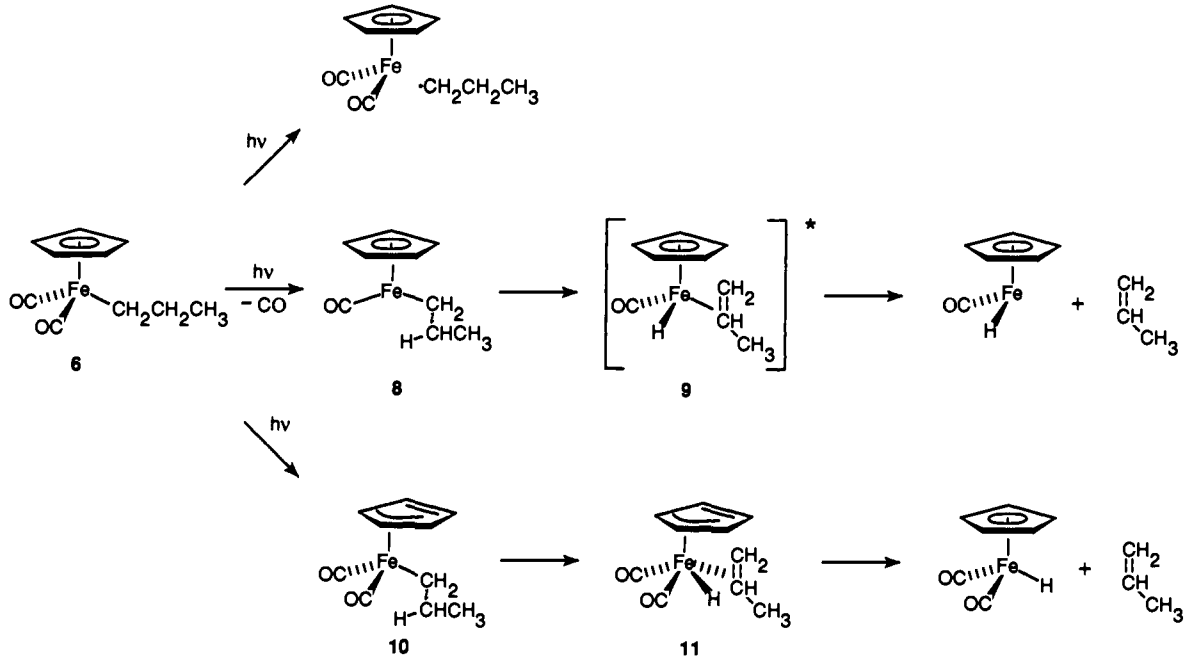

required to cleave either an Fe–CO bond (40 kcal/mol) or an Fe–alkyl bond (30 kcal/mol) (Table III). In fact, several bonds may break upon absorption of a single 280-nm photon. We can provide a rough estimate of the energetics for the two fragmentation processes using the approximate bond dissociation energies contained in Table III. For fragmentation reaction 1, $\Delta H \approx 110$ kcal/mol, and for fragmentation reaction 2, $\Delta H \approx 95$ kcal/mol.

$$CpFe(CO)_2CH_2CH_2CH_3 \longrightarrow CpFe + 2\,CO + CH_2CH_2CH_3 \quad (1)$$
$$\Delta H = 2\,D(Fe\text{-}CO) + D(Fe\text{-}C) = 110 \text{ kcal mol}^{-1}$$

$$CpFe(CO)_2CH_2CH_2CH_3 \longrightarrow CpFeH + 2\,CO + CH_2{=}CHCH_3 \quad (2)$$
$$\Delta H = 2\,D(Fe\text{-}CO) + D(Fe\text{-}C) + D(C\text{-}H) - D(Fe\text{-}H) - D(C{=}C) = 95 \text{ kcal mol}^{-1}$$

Given the relatively large uncertainty for some of the bond strengths in Table III, both fragmentation processes are thermodynamically possible upon photoexcitation at 280 nm (102 kcal/mol). If extensive fragmentation does occur, little energy remains for translational kinetic energy of the products. In fact, we know that the energy available to the photolysis fragments does not appear in relative translation. Analysis of the shapes of the features in the mass spectrum, which provides an estimate of the translational energy of the fragments,[68,69] shows that the alkyl translational energy is only (0.10 ± 0.02) eV and that of the alkene is only (0.06 ± 0.01) eV. Although the uncertainties in the bond energies make it difficult to assess the available energy, it is clear that very little appears in relative translation.

There are several possible mechanisms for the photofragmentation reactions we observe for complexes **1**, **6**, and **7**. One mechanism (Scheme II) postulates loss of CO, loss of alkyl radical, and ring slippage from η^5 to η^3 as competing photoprocesses. Cleavage of the metal–alkyl bond yields the alkyl radical, which we detect since in the gas phase it cannot recombine with $CpFe(CO)_2$. In competition with this, loss of CO or ring slippage generates coordinatively unsaturated intermediates (**8** or **10**, respectively), which could undergo β-hydride elimination. Using the bond dissociation energies in Table III, we estimate that β-hydride elimination (**8** → **9** or **10** → **11**) is exothermic by ca. 15 kcal/mol. In this mechanism, the excess internal energy present in hydrides **9** or **11** (ca. 70 kcal/mol) leads to loss of the alkene ligand that we observe.

We photolyzed the indenyl compound, $InFe(CO)_2CH_2CH_2CH_3$ (**7**), to investigate the role of the ring system in the branching between alkyl and alkene channels. The indenyl ligand undergoes ring slippage (η^5-In to η^3-In) to produce a vacant coordination site more readily than a cyclopentadienyl ligand, since resonance

energy from the attached 6-membered ring stabilizes the η^3 intermediate **12**.[70] A significant increase in propene signal compared to that of the propyl radical would indicate that the ring system helps generate a vacant site for β-hydride insertion. Comparison of the mass spectra of **6** and **7** (Figures 4 and 5) shows insignificant differences in the relative amounts of propyl and propene, (1.5 ± 0.8):1 for **6** and (1.1 ± 0.6):1 for **7**. The ring system has little effect on the branching ratio. The small differences in the branching for the cyclopentadienyl compound **6** and the indenyl compound **7** suggest that η^5 to η^3 ring slippage does not compete with other pathways that produce alkyl radical and alkene.[71–73]

A second mechanism (Scheme III) derives all the products from initial loss of CO. Since $CpFe(CO)CH_2CH_2CH_3$ (**8**) could

(68) Bartz, J. A. Ph.D. Thesis, University of Wisconsin-Madison, 1992.
(69) Penn, S. M.; Hayden, C. C.; Carlson-Muyskens, K. J.; Crim, F. F. *J. Chem. Phys.* **1988**, *89*, 2909–2917.

(70) In associative thermal reactions, the rate of ligand substitution increases up to 8 orders of magnitude, compared to that of the corresponding cyclopentadienyl compound: (a) Rerek, M. E.; Ji, L. N.; Basolo, F. *J. Chem. Soc., Chem. Commun.* **1983**, 1208–1209. (b) O'Connor, J. M.; Casey, C. P. *Chem. Rev.* **1987**, *87*, 307–318. (c) Casey, C. P.; O'Connor, J. M. *Organometallics* **1985**, *4*, 384–388.
(71) Various experimental observations are plausibly interpreted in terms of photochemical ring slippage, but direct observation of the process is lacking. Rest et al. found that both $InIr(CO)_2$ and $CpIr(CO)_2$ photochemically dissociate a carbonyl ligand prior to C–H bond activation of methane at 12 K.[72] Recently, Lees and co-workers reported that photoreactions of $(\eta^5\text{-}C_5H_5)M(CO)_2$ (M = Rh, Ir) involve associative mechanisms, possibly by η^5-to-η^3 ring slippage.[73] Further, they believe that a rigid matrix suppresses η^5-to-η^3 ring slippage.
(72) Rest, A. J.; Whitwell, I.; Graham, W. A. G.; Hoyano, J. K.; McMaster, A. D. *J. Chem. Soc., Dalton Trans.* **1987**, 1181–1190.
(73) (a) Marx, D. E.; Lees, A. J. *Inorg. Chem.* **1988**, *27*, 1121–1122. (b) Drolet, D. P.; Lees, A. J. *J. Am. Chem. Soc.* **1990**, *112*, 5878–5879. (c) Drolet, D. P.; Lees, A. J. *J. Am. Chem. Soc.* **1992**, *114*, 4186–4194.

Scheme III

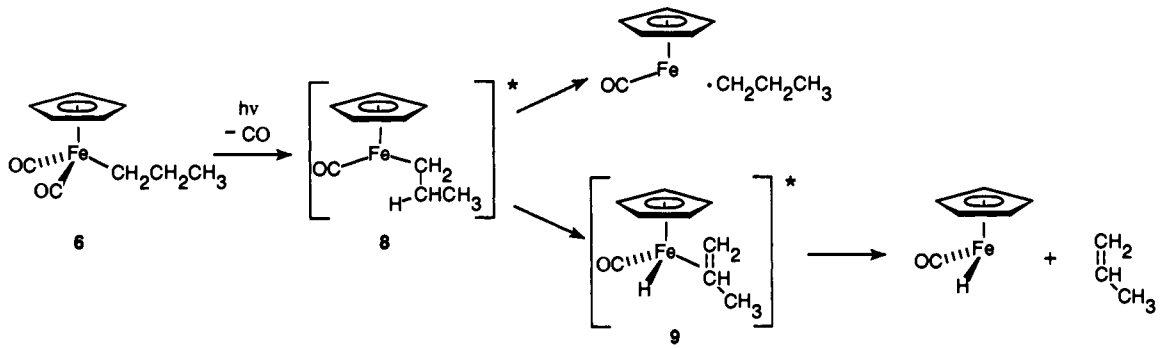

Scheme IV

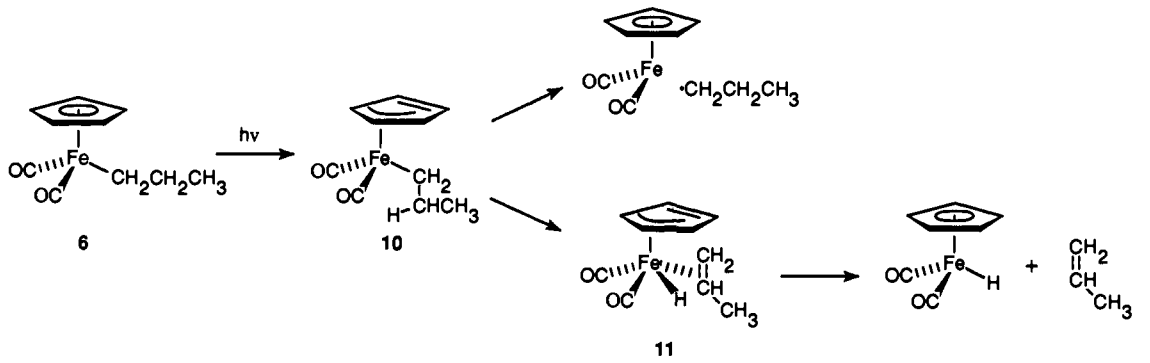

be formed with ca. 60–70 kcal/mol excess internal energy, it could cleave the metal–alkyl bond (30 kcal/mol) to produce a radical, which cannot recombine with CpFe(CO) in the gas phase. Alternatively, CpFe(CO)$CH_2CH_2CH_3$ (**8**) could undergo β-hydride insertion to yield **9**. Again, we assume that excess vibrational energy leads to loss of the alkene ligand. This mechanism does not involve ring-slipped intermediates at any stage, and is thus consistent with our observation of the similar reactivity for cyclopentadienyl complex **6** and indenyl complex **7**.

A third mechanism (Scheme IV) is analogous to the mechanism in Scheme III, except all products arise from initial ring-slippage of the cyclopentadienyl ligand, rather than initial loss of CO. Ring slippage from η^5-Cp to η^3-Cp generates a coordinatively unsaturated intermediate **10**, which possesses excess vibrational energy. This intermediate could partition between metal–alkyl bond homolysis to form an alkyl radical and β-hydride insertion to form hydride **11**. In **11**, ring slippage from η^3 back to η^5 could then occur with concomitant loss of alkene. In this mechanism, CO loss does *not* occur as a primary photochemical event; it occurs in vibrationally-excited ground state intermediates. Although this situation may seem unlikely, our data do not allow us to unequivocally rule it out. This mechanism is consistent with our results for the indenyl complex **7**, requiring only that ring-slipped intermediates **10** and **12** show similar partitioning between metal–alkyl bond homolysis and β-hydride insertion.

Again, we emphasize the ambiguity about the timing of CO loss. Each intermediate may actually contain fewer carbonyl ligands than shown in Schemes II–IV. The mechanisms in Scheme II (minus the ring-slippage pathway) and Scheme III straightforwardly accommodate our data. The mechanism in Scheme IV seems unlikely, but cannot be rigorously excluded.

Summary

We used vacuum ultraviolet photoionization mass spectrometry to identify the primary photoproducts of the photodissociation of a series of iron cyclopentadienyl compounds. The photolysis of these compounds isolated in a molecular beam produces comparable amounts of alkyl radicals and alkene. Dissociation of CpFe(CO)$_2CH_2CH_2CH_3$ (**6**) and InFe(CO)$_2CH_2CH_2CH_3$ (**7**) produces propyl radicals ($^{\bullet}CH_2CH_2CH_3$) and propene (CH_2=$CHCH_3$) in the ratio of (1.5 ± 0.8):1 and (1.1 ± 0.6):1, respectively. Both fragments carry away only a small amount of the available energy as relative translation. Alkene formation in these isolated molecules likely involves β-hydride elimination. We studied the indenyl compound **7**, which can undergo facile ring slippage (η^5 to η^3), to probe the role of the ring slippage in alkene formation. Replacing the cyclopentadienyl ring with an indenyl ring scarcely alters the relative amounts of propene and propyl radical, suggesting that ring slippage plays little role. The extensive photofragmentation we observe for **1**, **6**, and **7** contrasts with condensed phase results for the UV photolysis of **1**.

Acknowledgment. J.A.B. thanks the U.S. Department of Education for fellowship support, and T.G.M. gratefully acknowledges the support of the Alexander von Humboldt Foundation by a Feodor-Lynen Fellowship. R.J.M. thanks the National Science Foundation for a Presidential Young Investigator Award (1989–1994). We thank Carl R. Kemnitz for his critical reading of this manuscript. The Army Research Office and the National Science Foundation supported this work.